

---

# itKD: Interchange Transfer-based Knowledge Distillation for 3D Object Detection

---

Hyeon Cho, Junyong Choi, Geonwoo Baek, and Wonjun Hwang

Department of Artificial Intelligence

Ajou University

Suwon, Korea

{ch0104, ch1dusxkr, bkw0622, wjhwang}@ajou.ac.kr

## Abstract

Recently, point-cloud based 3D object detectors have achieved remarkable progress. However, most studies are limited to the development of deep learning architectures for improving only their accuracy. In this paper, we propose an autoencoder-style framework comprising channel-wise compression and decompression via interchange transfer for knowledge distillation. To learn the map-view feature of a teacher network, the features from a teacher and student network are independently passed through the shared autoencoder; here, we use a compressed representation loss that binds the channel-wised compression knowledge from both the networks as a kind of regularization. The decompressed features are transferred in opposite directions to reduce the gap in the interchange reconstructions. Lastly, we present an attentive head loss for matching the pivotal detection information drawn by the multi-head self-attention mechanism. Through extensive experiments, we verify that our method can learn the lightweight model that is well-aligned with the 3D point cloud detection task and we demonstrate its superiority using the well-known public datasets Waymo and nuScenes.

## 1 Introduction

Convolutional neural network (CNN)-based 3D object detection methods using point cloud [13][35][36][42][46] have attracted wide attention based on their outstanding performance for self-driving cars. Recent CNN-based works have required more computational complexity to achieve higher precision under the wild situation. Some studies [23][36][42] have proposed methods to improve the speed of 3D object detection through which the non-maximum suppression (NMS) or anchor procedures are removed but the network parameters were still large for sustaining a good performance.

Knowledge distillation (KD) is one of the parameter compression techniques that can effectively train a compact student network through the guidance of a deep teacher network. Starting with Hinton’s work [9], many studies on KD [10][21][27][43] have transferred the discriminative teacher knowledge to the student network for classification tasks. From the viewpoint of the detection task, KD should be extended to the regression problem, including the object positions; is not easy to directly apply previous classification-based KD methods to the detection task. To alleviate this problem, KD methods for object detection have been developed for mimicking the output of the backbone network (*e.g.*, region proposal network) or individual detection heads [2][15][32]. Nevertheless, these methods have only been studied for detecting 2D image-based objects, and there is a limit to applying them to sparse 3D point cloud-based data that do not have object-specific colors but only position-based structure information.

Looking at the fundamental difference between 2D and 3D data, there is a large feature gap in that 2D object detection estimates object positions based on discriminative color information while 3D object detection performs this only from the relations of the point coordinates between the objects. Note that the number of point clouds constituting an object varies depending on the distances and presence of occlusions [41]. Another challenge in 3D object detection for KD is that, compared to 2D object detection, 3D object detection [4][6][42] has more detection head components such as heatmaps, 3D boxes, orientations, the 3D box size. These multiple detection heads are highly correlated with each other and represent different 3D characteristics. In this respect, when transferring the detection heads of the teacher network to the student network using KD, it is required to guide the distilled knowledge under the consideration of the correlation between the multiple detection head components.

In this paper, we propose a novel interchange transfer-based knowledge distillation (itKD) method designed for point-cloud based lightweight 3D object detection. Our itKD comprises two modules: a channel-wise autoencoder based on the interchange transfer of reconstructed knowledge and a relation-aware self-attention for multiple 3D detection heads. Through a channel-wise compressing and decompressing process, the interchange transfer-based autoencoder effectively represents the map-view features from the viewpoint of object detection. Specifically, the encoder provides an efficient representation by compressing the map-view feature in the channel direction to preserve the spatial position information of the 3D objects while excluding the sparsity and noises in the map-view feature. In the compressed domain, the learning of the student network is regularized by the compressed guidance of the teacher network. For transferring the interchange knowledge, the decoder of the student reconstructs the map-view feature under the guidance of the teacher network while the reconstruction of the teacher network is guided by the map-view feature of the student. As a result, the student network can learn how to represent the map-view feature of the teacher for the detection task. Furthermore, for refining the teacher’s object detection results as well as its representation, our relation-aware self-attention learns the kind of information that should be taught to the student network for improving the detection results by considering the intra-relation of the individual detection head and the inter-relation among the multiple detection heads.

In this way, we implement a unified KD framework to successfully learn the representation of the teacher network and detection results for the lightweight 3D point cloud object detection. We also conduct extensive ablation studies for thoroughly analyzing of our approach. The results reveal the outstanding potential of the approach for transferring distilled knowledge that can be utilized to improve the performance of 3D point cloud object detection models, with 2.44–3.16% mAPH gains for each class. Also, we obtain comparable performances to the well-known methods on the Waymo and the nuScenes validation set.

Our contributions are summarized as follows:

- For learning the 3D feature representation of the teacher network, we propose the channel-wise autoencoder regularized in the compressed domain and the interchange knowledge transfer method wherein the reconstructed features are validated by the opposite networks.
- For learning the 3D detection results of the teacher network, we suggest the relation-aware self-attention which can efficiently distill the detection knowledge under the consideration of the inter-relation and intra-relation of the multiple 3D detection heads.
- To the best of our knowledge, our work is the first attempt to reduce the parameters of point cloud-based 3D object detection. Additionally, we validate its superiority using two large datasets that reflect real-world driving conditions.

## 2 Related Works

### 2.1 3D Object Detection in Point Cloud

During the last few years, encouraged by the success of CNNs, the development of object detectors using CNNs is developing rapidly. Recently, many 3D object detectors have been studied and they can be briefly categorized by how they extract representations from point clouds; *e.g.*, grid-based [35][36][46][13][42], point-based [19][23][17][24][24][38] and hybrid-based [3][39][8][45][22] methods.

Vote3Deep [5] thoroughly exploited feature-centric voting to build CNNs to detect objects in point clouds natively. A 3D region proposal network (RPN) to learn objectness from geometric shapes

and object recognition network to extract geometric features in 3D and color features has been suggested [28]. The 3D fully convolutional network was applied to point cloud data for vehicle detection [14]. VoxelNet [46] designed an end-to-end trainable detector based on learning-based voxelization using fully connected layers. In [35], they encoded the point cloud by VoxelNet and used sparse convolution for fast detection. HVNet [40] fused the multi-scale voxel feature encoder at the point-wise level and projected into multiple pseudo-image feature maps for solving the various sizes of the feature map. In [25], they replaced the point cloud with a grid-based bird’s-eye view (BEV) RGB-map and utilized YOLOv2 to detect the 3D objects. PIXOR [36] converted the point cloud to a 3D BEV map and carried out real-time 3D object detection with an RPN-free single-stage based model. PP [13] utilized PointNet [20] to learn the representation of point clouds organized in vertical columns for fast 3D object detection. To improve on the performance of PP, [33] a pillar-based method that incorporated a cylindrical projection into multi-view feature learning was proposed. More recently, CenterPoint [42] was introduced as an anchor-free detector that predicted the center of an object using a PP or VoxelNet-based feature encoder. In this paper, we build the backbone network using CenterPoint because it is simple, near real-time, and achieves good performance in the wild.

## 2.2 Knowledge Distillation

KD is one of the methods used for compressing deep neural networks and its fundamental key is to imitate the knowledge extracted from the teacher network. Hinton et al. [9] performed a knowledge transfer using KL divergence; FitNet [21] proposed a method for teaching student networks by imitating intermediate layers, and in AT [43], the student network mimicked the attention map of the teacher network via attention transfer. On the other hand, TAKD [16] and DGKD [27] used multiple teacher networks for transferring more knowledge to the student network. RKD [18] proposed a method to define the relationship between the output of the teacher and student networks. CRD [30] leveraged the contrastive objectives for KD. Recently, some studies have been propose using the layers shared between the teacher and the student networks for KD. Specifically, in [37], KD was performed through softmax regression as the student and teacher networks shared the same classifier. IEKD [10] proposed a method to split the student network into inheritance and exploration parts and mimic the compact teacher knowledge through a shared latent feature space via an autoencoder.

Beyond its use in classification, KD for detection should transfer the regression knowledge regarding the position of the object to the student network. For this purpose, a KD for 2D object detection [15] was first proposed using feature map mimic learning. In [2], they transferred the detection knowledge of the teacher network using hint learning for a RPN, weighted cross-entropy loss for classification, and bound regression loss for regression. Recently, Wang et al. [32] proposed a KD framework for detection by utilizing the cross-location discrepancy of feature responses through fine-grained feature imitation.

As far as we know, there are no KD studies on point cloud-based 3D object detection so far. However, looking at similar studies on 3D knowledge transfer, LIGA-Stereo [7] utilized only the geometry-aware feature from LiDAR-based 3D detection models to guide the training of stereo-based 3D detectors. This was a trial to improve lower performance of a stereo-based 3D detector with the help of the LiDAR-based detector, not a study to conduct the lightweight point cloud-based 3D object detection. Object-DGCNN [34] proposed a NMS-free 3D object detection via dynamic graphs and a set-to-set distillation, a kind of network ensemble method, was used to improve the performance of 3D object detection. The proposed method has not been used so far to make a lightweight network by itself.

## 3 Methodology

### 3.1 Background

Generally, 3D point cloud object detection methods [13][46] utilize three components; a point cloud encoder, a backbone, and detection heads. The backbone network contains the most network parameters among the detector components for representing latent features for 3D objects. Therefore, we aim to construct the student network by reducing the channel size of the backbone network parameters for effective model compression.

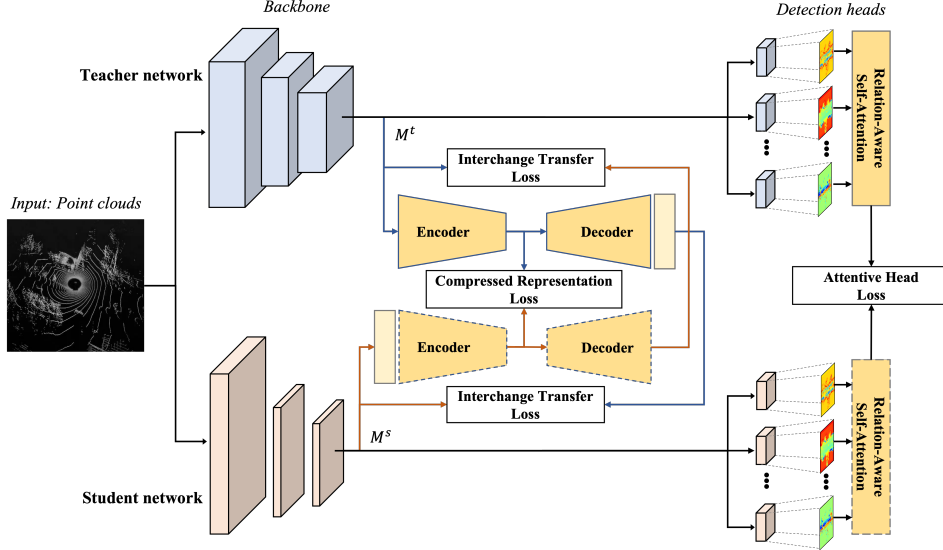


Figure 1: **Overview of the proposed knowledge distillation method.** The teacher and student networks take the same point clouds as inputs. Then, the map-view features  $M^t$  and  $M^s$  are extracted from the teacher and student network, respectively. The channel-wise autoencoder transfers the knowledge obtained from  $M^t$  to  $M^s$  by using the compressed representation loss and interchange transfer loss. The relation-aware self-attention provides the relation-aware knowledge of multiple detection heads to the student network using the attention head loss. The network parameters of the autoencoder and the relation-aware self-attention are shared between the teacher and student networks. The dotted lines of the modules denote that there are shared network parameters between the teacher and student networks. The light-yellow boxes are buffer layers for sampling the features to match the channel size.

### 3.2 Interchange Transfer for the backbone network

We adopt an autoencoder framework to effectively transfer the meaningful distilled knowledge for 3D detection from the teacher to the student network. The previous encoder-based methods for the classification task [10][11] only transferred the compressed categorical knowledge to the student network. Referring to the detection task, the main goal is not only limited to the classification task but also extended to both the classification and localization task, which they are different from each other. Particularly, unlike 2D detectors, 3D object detectors regress more values such as object orientation and 3D box size, increasing the burden on localization. To overcome this problem, we individually transfer categorical knowledge (*i.e.*, class of an object) and regressive knowledge (*i.e.*, 3D box size and object orientation) to the student network. For this purpose, as depicted in Fig. 1, we introduce a channel-wise autoencoder to transfer the categorical and regressive knowledge, which consists of an encoder in which the channel dimension of the autoencoder is gradually decreased and a decoder in the form of increasing the channel dimension. Note that spatial dimension plays a pivotal role in detection tasks.

At first, for transferring the categorical knowledge from the teacher to the student networks, we propose a compressed representation loss. As shown in Fig. 1, the compressed representation loss is coarsely a regularization that binds the key detection features of the teacher and student networks. The compressed representation loss function  $\mathcal{L}_{cr}$  is represented as follows:

$$\mathcal{L}_{cr} = \mathcal{S}[E(\theta_{enc}, M^t), E(\theta_{enc}, M^s)] = \mathcal{S}[M_{enc}^t, M_{enc}^s], \quad (1)$$

where  $E$  is a shared encoder, which has the parameters  $\theta_{enc}$  and  $\mathcal{S}$  denotes  $l_1$  loss as the similarity measure.  $M^t$  and  $M^s$  are outputs of the teacher and student backbones, respectively.

After performing a coarse knowledge distillation in a compressed domain, fine features, *e.g.*, 3D box sizes and orientations, of the teacher network are required to teach the student network from the viewpoint of 3D object detection. In this respect, the decoder decompresses the encoded feature in the channel direction to recover the fine map-view features. Through the proposed interchange transfer loss, the reconstructed features are guided from the opposite networks, not their own stem networks,

as shown in Fig. 1. Specifically, the reconstructed feature from the student network is directly guided from the output of the teacher network and the student network guides the teacher’s reconstructed feature distilling the regressive knowledge to both the networks simultaneously. During this time, the teacher network was frozen. We use the shared autoencoder for the student and teacher networks because, in the end, the teacher and student should produce almost similar results in detection. The proposed interchange transfer loss  $\mathcal{L}_{it}$  is defined as follows:

$$\mathcal{L}_{t2s} = \mathcal{S}[M^s, D(\theta_{dec}, M_{enc}^t)], \quad (2)$$

$$\mathcal{L}_{s2t} = \mathcal{S}[M^t, D(\theta_{dec}, M_{enc}^s)], \quad (3)$$

$$\mathcal{L}_{it} = \mathcal{L}_{s2t} + \mathcal{L}_{t2s}, \quad (4)$$

where  $D$  is the decoder that contains the network parameter  $\theta_{dec}$ , which is also a shared parameters.

We present a proper representation-based KD for 3D object detection in both the compressed and decompressed domains to guide the student network to mimic the map-view feature of the teacher network successfully.

### 3.3 Relation-Aware Self-Attention for Multiple Detection Heads

Our backbone network, *e.g.*, CenterPoint [42], has multiple detection heads specific to 3D object detection. Multiple detection heads perform different tasks but operate like a single module because they are configured to extract 3D object information from the same feature. However, the previous KD methods [2][34] were only concerned with how the student network directly mimicked the results of the teacher networks in detections, without completely considering the relation among the multiple detection heads. To alleviate this issue, we use the relation of multiple detection heads as a factor of KD in this paper.

Our proposed relation-aware self-attention is directly inspired by multi-head self-attention [31]. We extract a feature sequence  $v \in \mathbb{R}^{L \times C}$ , where  $C$  is the channel size of  $v$  and  $L$  is the number of objects in  $v$ . We use it as the query, key, and value. The feature sequence  $v$  refers to the aggregated features of objects corresponding to the actual location where objects exist in the output of the detection heads.  $v$  consists of a heatmap feature sequence  $v_{hm}$ , a subvoxel refinement feature sequence  $v_o$ , a height feature sequence  $v_h$ , a 3D size feature sequence  $v_s$ , and a rotation angle feature sequence  $v_r$ . We also develop an additional feature sequence  $v_{all}$  wherein all the feature sequences are concatenated on the channel direction.

Fig. 2 illustrates the relation-aware self-attention. It consists of the intra-relation attention and the inter-relation attention, which takes  $v_{all}$  and finds the correlation between multiple detection heads by applying self-attention to indicate which tasks of the detection heads take attention from the objects. Conversely, the other feature sequences  $v$  are processed by the intra-relation that suggests which objects are being noticed by the tasks of the detection heads. The fusion layer combines two results to calculate an attention score that considers the correlation between the tasks of the detection heads and objects. The relation-aware self-attention can be derived by:

$$\mathcal{F}(v) = softmax\left(\frac{v^T \cdot v}{\sqrt{L}}\right) \cdot v, \quad (5)$$

$$\mathcal{F}_{inter}(v) = [\mathcal{F}(v_{hm}), \mathcal{F}(v_o), \mathcal{F}(v_h), \mathcal{F}(v_s), \mathcal{F}(v_r)], \quad (6)$$

$$\mathcal{F}_{intra}(v) = \mathcal{F}([v_{hm}, v_o, v_h, v_s, v_r]), \quad (7)$$

$$\mathcal{F}_{RA}(v) = \mathcal{G}([\mathcal{F}_{inter}(v), \mathcal{F}_{intra}(v)]), \quad (8)$$

where  $\mathcal{F}$  is the self-attention,  $\mathcal{F}_{inter}$  is the inter-relation attention,  $\mathcal{F}_{intra}$  is the intra-relation attention,  $\mathcal{F}_{RA}$  is the relation-aware self-attention,  $\mathcal{G}$  is the fusion layer which is a  $1 \times 1$  convolution layer,  $L$  is the length of the feature sequence, and the sequences in the bracket are concatenated on the channel direction. The student network indirectly takes knowledge by mimicking the relation between the multiple detection heads of the teacher network through attentive head loss as follows:

$$\mathcal{L}_{attn} = \mathcal{S}[\mathcal{F}_{RA}(v^t), \mathcal{F}_{RA}(v^s)], \quad (9)$$

where  $v^t$  is the feature sequence of the teacher network, and  $v^s$  is the feature sequence of the student network.

Consequently, the overall loss is  $\mathcal{L}_{total} = \alpha \mathcal{L}_{sup} + \beta (\mathcal{L}_{it} + \mathcal{L}_{cr} + \mathcal{L}_{attn})$ , where  $\mathcal{L}_{sup}$  is the supervised loss that consists of focal loss and regression loss, and  $\alpha$  and  $\beta$  are the balancing parameters, which we set as 1 for simplicity.

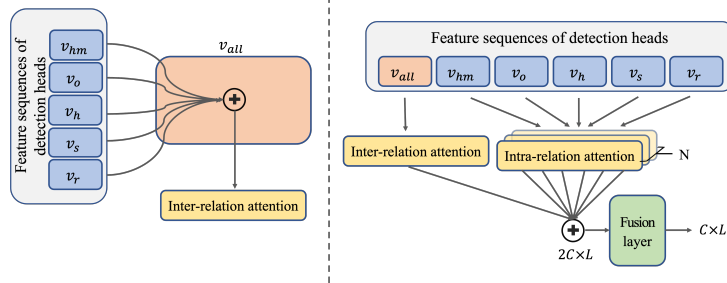


Figure 2: **Left:** The self-attention reveals the connection among multiple detection heads from  $v_{all}$ . **Right:** The overview of the relation-aware self-attention. Each self-attention for an individual detection head discovers the connection among the objects in the task from each  $v_{task}$ . Outputs of self-attentions are generated through the fusion layer.

## 4 Experiments

### 4.1 Environment Settings

**Waymo** The Waymo open dataset [29] is one of the large-scale datasets for autonomous driving, consisting of synchronized and calibrated high-quality LiDAR and camera data captured across a range of urban and suburban geographies. This dataset provides 798 training scenes and 202 validation scenes obtained from detecting all the objects within a 75m radius; it has a total of 3 object categories, namely vehicle, pedestrian, and cyclist, which have 6.1M, 2.8M, and 67K sets, respectively. We set the detection range to  $[-74.88m, 74.88m]$  for the X and Y axes and  $[-2m, 4m]$  for the Z-axis. The size of the voxel grid that we used was  $(0.32m, 0.32m)$ .

**nuScenes** The nuScenes dataset [1] is another large-scale dataset used for autonomous driving. This dataset contains 1,000 driving sequences. 700, 150, and 150 sequences are used for training, validation, and testing, respectively. Each sequence is captured approximately 20 seconds with 20 FPS using the 32-lane LiDAR. Its evaluation metrics are the average precision (AP) and nuScenes detection score (NDS). The NDS is a weighted average of the mean average precision (mAP) and other evaluation metrics for translation, scale, orientation, velocity, and other box attributes. In our experiments, we used a  $(0.2m, 0.2m)$  voxel grid and set the detection range to  $[-51.2m, 51.2m]$  for the X and Y-axes and  $[-5m, 3m]$  for the Z-axis.

**Implementation details** Following the use of CenterPoint [42] as the teacher network, we use an Adam optimizer [12] with a weight decay of 0.01 and a cosine annealing strategy [26] to adjust the learning rate. We set the initial learning rate at 0.003 and 0.95 for momentum. The networks have been trained for 36 epochs on  $8 \times V100$  GPUs with a batch size of 32. We use PointPillars [13] to encode the point clouds. In this paper, compared to the teacher network, the student network have 1/4 and 1/2 less filters of each layer for Waymo and nuScenes, respectively, because we evaluate the generality of our method for the different student architectures but the other detection components are identical to the teacher network. Our channel-wise autoencoder consists of three  $1 \times 1$  convolution layers as the encoder and three  $1 \times 1$  convolution layers as the decoder and the number of filters are 128, 64, 32 in encoder layers and 64, 128, 384 in decoder layers. The student’s input buffer layer increases the channel size of 196 to 384 and the teacher’s output buffer layer decreases the channel size 384 to 196.

### 4.2 Overall KD Performance

We compare the performance of our method with those of well-known KD methods on the Waymo and nuScenes datasets to validate it. Specifically, we reimplement the following KD methods; Hinton’s KD [9] and FitNet [21], which are mainly used in KD for 2D classification, EOD-KD [2] that is used for 2D object detection KD, and TOFD [44] and Object DGCNN [34] used for 3D object detection KD. We set the baseline by applying the Kullback-Leibler (KL) divergence loss to the heatmap head and  $l_1$  loss to the other detection heads. FitNet is a method that mimics the intermediate outputs of layers and we apply it to the output of the backbone for simplicity. EOD-KD employed the hint loss to the output of the backbone, the weighted cross-entropy loss to the heatmap head, and the bounded

Table 1: Comparisons with different KD methods in the Waymo validation set. The best accuracy is indicated in bold, and the second-best accuracy is underlined.

Method	Vehicle				Pedestrian				Cyclist			
	Level 1		Level 2		Level 1		Level 2		Level 1		Level 2	
	mAP	mAPH										
Teacher [42]	73.00	72.43	64.89	64.37	72.01	61.57	64.29	54.79	63.30	61.51	60.93	59.20
Student	64.22	63.56	56.21	55.62	63.72	53.22	56.14	46.78	53.01	51.72	50.99	49.75
Baseline [9]	64.78	64.05	56.92	56.26	64.85	52.98	57.37	46.75	54.71	52.46	52.65	50.48
FitNet [21]	65.11	64.38	57.24	56.58	64.89	53.29	57.37	47.00	54.91	52.61	52.84	50.63
EOD-KD [2]	<u>66.50</u>	65.79	58.56	57.92	65.99	54.58	58.48	48.25	<u>55.18</u>	52.93	53.10	50.94
TOFD [44]	64.09	63.43	56.13	55.55	<u>66.24</u>	54.98	58.50	48.45	54.95	<u>53.06</u>	52.86	<u>51.04</u>
Obj. DGCNN [34]	66.07	<u>65.38</u>	<u>59.27</u>	<u>58.55</u>	65.98	54.44	<u>59.42</u>	<u>49.11</u>	54.65	52.62	<u>53.13</u>	50.93
Ours	<b>67.43</b>	<b>66.72</b>	<b>59.44</b>	<b>58.81</b>	<b>67.26</b>	<b>56.02</b>	<b>59.73</b>	<b>49.61</b>	<b>56.09</b>	<b>54.24</b>	<b>53.96</b>	<b>52.19</b>

Table 2: Comparisons with different KD methods in the nuScenes validation set. The best accuracy is indicated in bold, and the second-best accuracy is underlined.

Method	NDS	mAP	car	truck	bus	trailer	con. veh.	ped.	motor.	bicycle	tr. cone	barrier
Teacher [42]	59.45	48.83	83.64	48.97	60.88	32.60	10.57	77.50	42.60	15.07	55.58	60.84
Student	56.79	45.45	82.10	45.00	60.60	27.80	7.40	76.80	35.30	9.90	52.80	56.80
Baseline [9]	57.95	46.78	<u>82.70</u>	<b>47.10</b>	<b>61.00</b>	28.20	8.20	77.60	<b>39.80</b>	11.70	53.20	58.30
FitNet [21]	57.97	46.90	82.60	46.20	60.00	28.80	8.70	<u>77.90</u>	<u>39.20</u>	<u>14.20</u>	52.90	58.50
EOD-KD [2]	<u>58.07</u>	46.83	<u>82.70</u>	46.80	<u>60.80</u>	29.00	8.70	77.60	39.10	11.60	<u>53.40</u>	58.60
TOFD [44]	57.54	46.10	82.50	46.20	59.50	29.00	7.30	77.20	38.70	13.00	51.60	56.00
Obj. DGCNN [34]	57.96	<u>46.92</u>	82.60	46.10	59.10	<u>29.20</u>	<b>9.20</b>	77.60	38.60	<u>14.20</u>	<u>53.40</u>	<b>59.20</b>
Ours	<b>58.32</b>	<b>47.18</b>	<b>82.91</b>	47.05	59.04	<b>29.80</b>	9.08	<b>78.03</b>	38.61	<b>15.09</b>	<b>53.56</b>	58.64

regression loss to the other heads. TOFD used the focal loss to reduce the difference with the output of the teacher network at the location where downsampling occurs in the backbone network. Object DGCNN is reimplemented by applying the focal loss to the heatmap head and  $l_1$  loss to the others for the KD task. CenterPoint [42] is mainly used as a backbone architecture for the teacher network.

We compare our performance on the Waymo dataset. mAP and the mean average precision weighted by heading (mAPH) are used as the evaluation metrics. mAPH is a metric that gives more weight to the heading than it does to the sizes, and it accounts for the direction of the object. Table 1 shows that our method outperforms other well-known KD methods significantly on mAP and mAPH values for level 1 and level 2 under all three categories of objects. Our performance particularly presents to be higher in improvement of mAPH than mAP. Overall, we confirm that our method shows better performance in transferring 3D object knowledge regarding the orientation of objects.

For verifying the generality of the proposed method, we make comparison results using the nuScenes detection task set, another large-scale 3D dataset for autonomous driving, in Table 2. Compared with the other methods, our method achieves the best accuracy under the NDS and mAP metrics in the nuScenes validation set. When the student network shows 56.79% NDS and 45.45% mAP, our method achieves 58.32% (+1.53%) NDS and 47.18% (+1.73%) mAP. In detail, our method outperforms the other methods for the car, trailer, pedestrian, bicycle, and traffic cones and it shows the second best performance for the trucks, construction vehicles, and barriers. That is, our method achieves the first and second performance in 8 out of 10 classes.

### 4.3 Ablation Studies

To analyze of our proposed method in greater detail, we conduct ablation studies on the Waymo dataset. Here, we use the mAPH performance of level 2 for simplicity.

Table 3: Buffer layer for different channels.

Method	Vehicle	Pedestrian	Cyclist
$S \rightarrow T$	58.41	<b>48.90</b>	<b>51.90</b>
$T \rightarrow S$	<b>58.62</b>	48.78	51.75
$(S + T) / 2$	58.47	48.84	51.54

Table 4: Effect of shared parameters of autoencoder.

Method	Vehicle	Pedestrian	Cyclist
Non-shared	56.26	45.85	48.23
Shared	<b>58.81</b>	<b>49.61</b>	<b>52.19</b>

In Table 3, we explore the buffer layer that matches the channel size of the channel-wise autoencoder without only the attentive head loss. We compare the three methods for the buffer layer: (1)  $S \rightarrow T$

is the upsampling method that increases the student’s map-view feature to the teacher’s feature. (2)  $T \rightarrow S$  is the downsampling method that decreases the teacher’s feature to the student’s feature. (3)  $(S + T) / 2$  is that the teacher’s feature is downsampled and the student’s feature is upsampled to the median size. The experiments reveal that the upsampling method shows a better performances when considering all the classes.

Next, we observe the effect of the shared parameters of the autoencoder. Table 4 illustrates the performance gap between the shared and non-shared autoencoder. In case of the non-shared autoencoder, the encoder and the decoder are not shared with each other and the other configurations are the same. As shown in the result, we observe that the shared parameters have a good performance because it helps to alleviate the difference between the autoencoders corresponding to the teacher and student networks.

Table 5: Comparisons of different reconstruction methods for the autoencoder.

Method	Vehicle	Pedestrian	Cyclist
Self-Recon.	56.57	47.26	50.29
Interchange Recon. (Ours)	<b>58.41</b>	<b>49.61</b>	<b>51.90</b>

Table 6: Comparison of KD methods for the multiple detection heads.

Method	Vehicle	Pedestrian	Cyclist
Baseline	56.26	46.75	50.48
Hinton	55.92	45.08	47.49
$l_1$ loss	55.62	45.10	48.73
$\mathcal{L}_{attn}$	<b>57.10</b>	<b>47.34</b>	<b>51.79</b>

We investigate improvements made by the proposed interchange transfer for KD without the attentive head loss as shown in Table 5. Self-reconstruction is a method wherein the decoder uses the corresponding input for the reconstruction and interchange reconstruction is a method wherein the proposed  $\mathcal{L}_{it}$  objective transfers the reconstructed knowledge to the opponent network. Our main task is KD, not reconstruction and the interchange of knowledge to each other results in a better performances.

Unlike 2D detection, 3D object detection [42] has multiple detection heads. For proving the superiority of the proposed attentive head objective for 3D object detection, we make the KD comparison results against only multiple detection heads, as shown in Table 6. Since our method fully considers the relation of each detection head, it achieves a better performance than the other KD methods that unilaterally teach the distilled knowledge to the student network.

Table 7: Ablation results from investigating effects of different components.

$\mathcal{L}_{sup}$	$\mathcal{L}_{it}$	$\mathcal{L}_{cr}$	$\mathcal{L}_{attn}$	Vehicle	Pedestrian	Cyclist	Avg.
✓				55.62	46.78	49.75	50.72
✓	✓			57.41	48.20	50.77	52.13
✓	✓	✓		58.41	48.90	51.90	53.07
✓	✓	✓	✓	<b>58.81</b>	<b>49.61</b>	<b>52.19</b>	<b>53.54</b>

Table 7 shows the effect of the proposed losses on the KD performances. We set up the experiments by adding each loss based on the supervised loss  $\mathcal{L}_{sup}$ . Specifically, the interchange transfer loss  $\mathcal{L}_{it}$  improves on an average of 1.41% mAPH and the compressed representation loss  $\mathcal{L}_{cr}$  leads to a 0.94% performance improvement. In the end, the attentive head loss  $\mathcal{L}_{attn}$  helps to improve the performance and the final average mAPH is 53.54%. We conclude that each proposed loss contributes positively to performance improvement in the 3D object detection-based KD task.

#### 4.4 Self-Distillation Performances

Table 8: Comparison of self-distillation results.

Method	Vehicle	Pedestrian	Cyclist
Teacher [42]	64.37	54.79	59.20
Obj. DGCNN [34]	65.13	<b>54.95</b>	59.79
Ours	<b>65.24</b>	<b>54.95</b>	<b>60.12</b>

We compare the proposed method to that with the teacher network and the Object DGCNN [34] with the self-distillation protocol, not KD. Self-distillation is a method to distill knowledge within just the network; it is more a learning method that boosts model performance rather than a method that compresses models. As shown in Table 8, our method still achieves better results for the whole class compared with the Object DGCNN and the teacher network. From this result, we conclude that the proposed method has the potential capacity to produce to good results in any kind of 3D object task.

## 5 Conclusion

In this paper, we propose a novel KD method that transfers 3D knowledge to produce a lightweight point cloud detector. Our main method involves interchange transfer, which mimics knowledge by decompressing the map-view feature of the other side using the channel-wise autoencoder and the compressed representation loss, which regularizes the autoencoder by increasing the similarity of the encoded feature. Moreover, we have introduced a method to indirectly guide multiple detection heads using relation-aware self-attention, which refines knowledge by considering the relationships between objects and detection head tasks. Ablation studies demonstrate the effectiveness of our proposed algorithm, and extensive experiments on the two large-scale open datasets verify that our proposed method achieves competitive performances to the state-of-the-art methods.

**Limitation.** We note that using the autoencoder often requires additional effort for propoely identifying the proper network structure or its hyper-parameters for the different 3D object detection. We believe that the deviations of the hyper-parameters are not high.

**Potential impact.** Our KD method aims to make an efficient 3D object detection network, which is crucial for the autonomous driving system that requires real-time response. One potential negative impact of our method is that the quantitative performance of the student network follows similarly to that of the teacher network; also, it has not been confirmed whether there are any parts that can be fatal to the safety of the autonomous driving system in the wild.

## References

- [1] Holger Caesar, Varun Bankiti, Alex H Lang, Sourabh Vora, Venice Erin Liong, Qiang Xu, Anush Krishnan, Yu Pan, Giancarlo Baldan, and Oscar Beijbom. nuscenes: A multimodal dataset for autonomous driving. In *Proceedings of the IEEE/CVF conference on computer vision and pattern recognition*, pages 11621–11631, 2020.
- [2] Guobin Chen, Wongun Choi, Xiang Yu, Tony Han, and Manmohan Chandraker. Learning efficient object detection models with knowledge distillation. *Advances in neural information processing systems*, 30, 2017.
- [3] Yilun Chen, Shu Liu, Xiaoyong Shen, and Jiaya Jia. Fast point r-cnn. In *Proceedings of the IEEE/CVF International Conference on Computer Vision*, pages 9775–9784, 2019.
- [4] Xiyang Dai, Yinpeng Chen, Bin Xiao, Dongdong Chen, Mengchen Liu, Lu Yuan, and Lei Zhang. Dynamic head: Unifying object detection heads with attentions. In *Proceedings of the IEEE/CVF Conference on Computer Vision and Pattern Recognition*, pages 7373–7382, 2021.
- [5] Martin Engelcke, Dushyant Rao, Dominic Zeng Wang, Chi Hay Tong, and Ingmar Posner. Vote3deep: Fast object detection in 3d point clouds using efficient convolutional neural networks. In *2017 IEEE International Conference on Robotics and Automation (ICRA)*, pages 1355–1361. IEEE, 2017.
- [6] Runzhou Ge, Zhuangzhuang Ding, Yihan Hu, Yu Wang, Sijia Chen, Li Huang, and Yuan Li. Afdet: Anchor free one stage 3d object detection. *arXiv preprint arXiv:2006.12671*, 2020.
- [7] Xiaoyang Guo, Shaoshuai Shi, Xiaogang Wang, and Hongsheng Li. Liga-stereo: Learning lidar geometry aware representations for stereo-based 3d detector. In *Proceedings of the IEEE/CVF International Conference on Computer Vision*, pages 3153–3163, 2021.
- [8] Chenheng He, Hui Zeng, Jianqiang Huang, Xian-Sheng Hua, and Lei Zhang. Structure aware single-stage 3d object detection from point cloud. In *Proceedings of the IEEE/CVF Conference on Computer Vision and Pattern Recognition*, pages 11873–11882, 2020.
- [9] Geoffrey Hinton, Oriol Vinyals, Jeff Dean, et al. Distilling the knowledge in a neural network. *arXiv preprint arXiv:1503.02531*, 2(7), 2015.

- [10] Zhen Huang, Xu Shen, Jun Xing, Tongliang Liu, Xinmei Tian, Houqiang Li, Bing Deng, Jianqiang Huang, and Xian-Sheng Hua. Revisiting knowledge distillation: An inheritance and exploration framework. In *Proceedings of the IEEE/CVF Conference on Computer Vision and Pattern Recognition*, pages 3579–3588, 2021.
- [11] Jangho Kim, SeongUk Park, and Nojun Kwak. Paraphrasing complex network: Network compression via factor transfer. *Advances in neural information processing systems*, 31, 2018.
- [12] Diederik P Kingma and Jimmy Ba. Adam: A method for stochastic optimization. *arXiv preprint arXiv:1412.6980*, 2014.
- [13] Alex H Lang, Sourabh Vora, Holger Caesar, Lubing Zhou, Jiong Yang, and Oscar Beijbom. Pointpillars: Fast encoders for object detection from point clouds. In *Proceedings of the IEEE/CVF Conference on Computer Vision and Pattern Recognition*, pages 12697–12705, 2019.
- [14] Bo Li. 3d fully convolutional network for vehicle detection in point cloud. In *2017 IEEE/RSJ International Conference on Intelligent Robots and Systems (IROS)*, pages 1513–1518. IEEE, 2017.
- [15] Quanquan Li, Shengying Jin, and Junjie Yan. Mimicking very efficient network for object detection. In *Proceedings of the IEEE conference on computer vision and pattern recognition*, pages 6356–6364, 2017.
- [16] Seyed Iman Mirzadeh, Mehrdad Farajtabar, Ang Li, Nir Levine, Akihiro Matsukawa, and Hassan Ghasemzadeh. Improved knowledge distillation via teacher assistant. In *Proceedings of the AAAI Conference on Artificial Intelligence*, pages 5191–5198, 2020.
- [17] Jiquan Ngiam, Benjamin Caine, Wei Han, Brandon Yang, Yuning Chai, Pei Sun, Yin Zhou, Xi Yi, Ouais Alsharif, Patrick Nguyen, et al. Starnet: Targeted computation for object detection in point clouds. *arXiv preprint arXiv:1908.11069*, 2019.
- [18] Wonpyo Park, Dongju Kim, Yan Lu, and Minsu Cho. Relational knowledge distillation. In *Proceedings of the IEEE/CVF Conference on Computer Vision and Pattern Recognition*, pages 3967–3976, 2019.
- [19] Charles R Qi, Wei Liu, Chenxia Wu, Hao Su, and Leonidas J Guibas. Frustum pointnets for 3d object detection from rgb-d data. In *Proceedings of the IEEE conference on computer vision and pattern recognition*, pages 918–927, 2018.
- [20] Charles R Qi, Hao Su, Kaichun Mo, and Leonidas J Guibas. Pointnet: Deep learning on point sets for 3d classification and segmentation. In *Proceedings of the IEEE conference on computer vision and pattern recognition*, pages 652–660, 2017.
- [21] Adriana Romero, Nicolas Ballas, Samira Ebrahimi Kahou, Antoine Chassang, Carlo Gatta, and Yoshua Bengio. Fitnets: Hints for thin deep nets. *arXiv preprint arXiv:1412.6550*, 2014.
- [22] Shaoshuai Shi, Chaoxu Guo, Li Jiang, Zhe Wang, Jianping Shi, Xiaogang Wang, and Hongsheng Li. Pv-rcnn: Point-voxel feature set abstraction for 3d object detection. In *Proceedings of the IEEE/CVF Conference on Computer Vision and Pattern Recognition*, pages 10529–10538, 2020.
- [23] Shaoshuai Shi, Xiaogang Wang, and Hongsheng Li. Pointtrnn: 3d object proposal generation and detection from point cloud. In *Proceedings of the IEEE/CVF conference on computer vision and pattern recognition*, pages 770–779, 2019.
- [24] Weijing Shi and Raj Rajkumar. Point-gnn: Graph neural network for 3d object detection in a point cloud. In *Proceedings of the IEEE/CVF conference on computer vision and pattern recognition*, pages 1711–1719, 2020.
- [25] Martin Simony, Stefan Milzy, Karl Amendey, and Horst-Michael Gross. Complex-yolo: An euler-region-proposal for real-time 3d object detection on point clouds. In *Proceedings of the European Conference on Computer Vision (ECCV) Workshops*, pages 0–0, 2018.
- [26] Leslie N Smith. Cyclical learning rates for training neural networks. In *2017 IEEE winter conference on applications of computer vision (WACV)*, pages 464–472. IEEE, 2017.
- [27] Wonchul Son, Jaemin Na, Junyong Choi, and Wonjun Hwang. Densely guided knowledge distillation using multiple teacher assistants. In *Proceedings of the IEEE/CVF International Conference on Computer Vision*, pages 9395–9404, 2021.

- [28] Shuran Song and Jianxiong Xiao. Deep sliding shapes for amodal 3d object detection in rgb-d images. In *Proceedings of the IEEE conference on computer vision and pattern recognition*, pages 808–816, 2016.
- [29] Pei Sun, Henrik Kretzschmar, Xerxes Dotiwalla, Aurelien Chouard, Vijaysai Patnaik, Paul Tsui, James Guo, Yin Zhou, Yuning Chai, Benjamin Caine, et al. Scalability in perception for autonomous driving: Waymo open dataset. In *Proceedings of the IEEE/CVF conference on computer vision and pattern recognition*, pages 2446–2454, 2020.
- [30] Yonglong Tian, Dilip Krishnan, and Phillip Isola. Contrastive representation distillation. *arXiv preprint arXiv:1910.10699*, 2019.
- [31] Ashish Vaswani, Noam Shazeer, Niki Parmar, Jakob Uszkoreit, Llion Jones, Aidan N Gomez, Łukasz Kaiser, and Illia Polosukhin. Attention is all you need. *Advances in neural information processing systems*, 30, 2017.
- [32] Tao Wang, Li Yuan, Xiaopeng Zhang, and Jiashi Feng. Distilling object detectors with fine-grained feature imitation. In *Proceedings of the IEEE/CVF Conference on Computer Vision and Pattern Recognition*, pages 4933–4942, 2019.
- [33] Yue Wang, Alireza Fathi, Abhijit Kundu, David A Ross, Caroline Pantofaru, Tom Funkhouser, and Justin Solomon. Pillar-based object detection for autonomous driving. In *European Conference on Computer Vision*, pages 18–34. Springer, 2020.
- [34] Yue Wang and Justin M Solomon. Object dgcnn: 3d object detection using dynamic graphs. *Advances in Neural Information Processing Systems*, 34, 2021.
- [35] Yan Yan, Yuxing Mao, and Bo Li. Second: Sparsely embedded convolutional detection. *Sensors*, 18(10):3337, 2018.
- [36] Bin Yang, Wenjie Luo, and Raquel Urtasun. Pixor: Real-time 3d object detection from point clouds. In *Proceedings of the IEEE conference on Computer Vision and Pattern Recognition*, pages 7652–7660, 2018.
- [37] Jing Yang, Brais Martinez, Adrian Bulat, and Georgios Tzimiropoulos. Knowledge distillation via softmax regression representation learning. In *International Conference on Learning Representations*, 2020.
- [38] Zetong Yang, Yanan Sun, Shu Liu, and Jiaya Jia. 3dssd: Point-based 3d single stage object detector. In *Proceedings of the IEEE/CVF conference on computer vision and pattern recognition*, pages 11040–11048, 2020.
- [39] Zetong Yang, Yanan Sun, Shu Liu, Xiaoyong Shen, and Jiaya Jia. Std: Sparse-to-dense 3d object detector for point cloud. In *Proceedings of the IEEE/CVF International Conference on Computer Vision*, pages 1951–1960, 2019.
- [40] Maosheng Ye, Shuangjie Xu, and Tongyi Cao. Hynet: Hybrid voxel network for lidar based 3d object detection. In *Proceedings of the IEEE/CVF conference on computer vision and pattern recognition*, pages 1631–1640, 2020.
- [41] Zeng Yihan, Chunwei Wang, Yunbo Wang, Hang Xu, Chaoqiang Ye, Zhen Yang, and Chao Ma. Learning transferable features for point cloud detection via 3d contrastive co-training. *Advances in Neural Information Processing Systems*, 34, 2021.
- [42] Tianwei Yin, Xingyi Zhou, and Philipp Krahenbuhl. Center-based 3d object detection and tracking. In *Proceedings of the IEEE/CVF conference on computer vision and pattern recognition*, pages 11784–11793, 2021.
- [43] Sergey Zagoruyko and Nikos Komodakis. Paying more attention to attention: Improving the performance of convolutional neural networks via attention transfer. *5th international conference on Learning Representations*, Apr. 2017.
- [44] Linfeng Zhang, Yukang Shi, Zuoqiang Shi, Kaisheng Ma, and Chenglong Bao. Task-oriented feature distillation. *Advances in Neural Information Processing Systems*, 33:14759–14771, 2020.
- [45] Yin Zhou, Pei Sun, Yu Zhang, Dragomir Anguelov, Jiyang Gao, Tom Ouyang, James Guo, Jiquan Ngiam, and Vijay Vasudevan. End-to-end multi-view fusion for 3d object detection in lidar point clouds. In *Conference on Robot Learning*, pages 923–932. PMLR, 2020.

- [46] Yin Zhou and Oncel Tuzel. Voxelnet: End-to-end learning for point cloud based 3d object detection. In *Proceedings of the IEEE conference on computer vision and pattern recognition*, pages 4490–4499, 2018.